JOURNAL OF GEOPHYSICAL RESEARCH, VOL. 102, NO. C11, PAGES 25,047–25,060, NOVEMBER 15, 1997

Sources of variability in the column photosynthetic cross section for Antarctic coastal waters

Hervé Claustre,[1] Mark A. Moline, and Barbara B. Prézelin

Department of Ecology, Evolution and Marine Biology, University of California at Santa Barbara

Abstract. Using a highly resolved Long Term Ecological Research (LTER) database collected near Palmer Station, Antarctica, from 1991 to 1994, the variability in the column photosynthetic cross section (Ψ^*, m^2 g Chl a^{-1}) was analyzed. The relationship between the daily integrated primary production rates versus the product of surface irradiance ($Q_{PAR}(0^+)$) and the integrated chlorophyll content (down to 0.1% $Q_{PAR}(0^+)$) gave a Ψ^* value of 0.0695 m^2 g Chl a^{-1} ($r^2 = 0.85$, $p < 0.001$, $n = 151$) which is similar to those determined for temperate and tropical seas. However, the average value of single Ψ^* estimates is higher (0.109 ± 0.075 m^2 g Chl a^{-1}) with extreme values extending over a fiftyfold range (0.009-0.488 m^2 g Chl a^{-1}). The possible drivers of this variability are analyzed in detail, considering variables which are presently used in biooptical models (e.g., surface irradiance and chlorophyll content) and those which are not (taxonomic composition). A sixfold variation in Ψ^* was observed with time of year and strongly associated with the high seasonality in incident irradiance characteristic of these polar sampling sites. Variability in daily incident irradiance as influenced by cloudiness and variation in chlorophyll content were responsible for an additional twofold variation in Ψ^*. Finally, the taxonomic dependency of Ψ^* was demonstrated for the first time. For identical chlorophyll content and surface irradiance, mean Ψ^* values of 0.114 ± 0.051 m^2 g Chl a^{-1} were recorded for diatom blooms and 0.053 ± 0.011 m^2 g Chl a^{-1} for cryptophyte-dominated populations. Results illustrate the validity of Ψ^*-based approaches for estimating primary production for the Southern Ocean but emphasize the need to address taxon-specific photophysiology to better estimate primary production on smaller spatio-temporal scales.

Introduction

Today, attempts to estimate primary production from space utilize algorithms which incorporate phytoplankton photophysiology [*Lewis*, 1992]. These algorithms are generally based upon a mechanistic understanding of the photosynthesis-irradiance (P-I) relationship [*Morel*, 1991; *Bidigare et al.*, 1992]. However, first attempts to derive primary production rates from variables which are determinable by remote sensing, namely surface irradiance and chlorophyll content, have relied on empirical relationships [e.g., *Morel*, 1978]. *Falkowski* [1981] postulated that daily integrated rates of primary production could be modeled as a direct function of the product of surface irradiance $Q_{PAR}(0^+)$ (mol quanta m^{-2} d^{-1}) and an estimate of areal chlorophyll a (g Chl a m^{-2}), through an efficiency factor called the column light utilization index Ψ (g C (g Chl a)$^{-1}$ m^2 (mol quanta)$^{-1}$) (see Table 1 for notation) :

$$\Psi = \frac{P}{Q_{PAR}(0^+)\langle Chl \rangle} \quad (1)$$

By expressing surface irradiance and primary production in energy equivalent, *Morel* [1978, 1991] proposed a similar index, Ψ^* (m^2 g Chl a^{-1}), the column photosynthetic cross section:

$$\Psi^* = \frac{39P}{Q_{PAR}(0^+)\langle Chl \rangle} \quad (2)$$

where the constant value of 39 corresponds to the kilojoules of chemical energy stored by the photosynthetic fixation of 1 g C and $Q_{PAR}(0^+)$ is expressed as energy (kJ m^{-2} d^{-1}). The conversion from Ψ to Ψ^* is achieved with a nondimensionless conversion factor, such that $\Psi = 6.174\ \Psi^*$ [*Morel*, 1991].

Morel [1978] and *Platt* [1986] reviewed various trophic situations in temperate and tropical oceans and observed that Ψ^* varies by ± 50 % (at 1 standard deviation) around a central value of 0.07 m^2 g Chl a^{-1}. Such an a priori consistency and stability for this biogeochemical index are of great hope in view of mapping primary production at a global scale. Recently, *Prasad et al.* [1995] estimated similar values for coastal waters of the Gulf of Mexico and *Claustre and Marty* [1995] have found comparable results for the tropical North Atlantic. However, higher and more variable values for Ψ^* were reported by *Campbell and O'Reilly* [1988] for the northwest Atlantic continental shelf, by *Siegel et al.* [1995] for the Bermuda Atlantic Time-Series study (BATS) and by *Balch and Byrne* [1994] for an analysis at a global scale. While experimental or analytical differences may explain the discrepancies in different estimates of Ψ^* [*Campbell and O'Reilly*, 1988; *Siegel et al.*, 1995], it is equally possible that systematic variations in Ψ^* do occur in nature. Understanding these sources of variability will lead to future development of more accurate remote-sensing algorithms. *Morel* [1991], using a modeling approach, addressed potential sources of variability in Ψ^* by documenting the effect of incident irradiance changes (mostly driven by latitude, seasonality, and cloudiness) as well as the effect of chlorophyll a variations (driven

[1] Also at Laboratoire de Physique et Chimie Marines, CNRS-INSU, Villefranche-sur-mer, France.

Paper number 96JC02439.
0148-0227/97/96JC-02439$09.00

Table 1. List of Symbols

Symbol	Definition	Units
$\bar{a}^{*}$ [a]	mean, reconstructed specific absorption coefficient	m^2 g Chl a^{-1}
$\bar{a}^{*}_{act}$ [a]	same as $\bar{a}^{*}$, but for photosynthetic (active) pigments only	m^2 g Chl a^{-1}
$\alpha(z)$	slope of the photosynthesis-light curve at depth z	(mg C m^{-3} h^{-1}) (µmol quanta m^{-2} s^{-1})$^{-1}$
$\bar{\alpha}^{B}$ [a]	mean, Chl-normalized $\alpha(z)$	(mg C mg Chl $a^{-1}h^{-1}$) (µmol quanta m^{-2} s^{-1})$^{-1}$
Chl(z)	Chlorophyll a concentration at depth z	mg Chl a m^{-3}
$\overline{\text{Chl}}$ [a]	mean Chl concentration	mg Chl a m^{-3}
<Chl> [a]	integrated Chl concentration	mg Chl a m^{-2}
P [a]	integrated daily primary production rates	g C m^{-2} d^{-1}
$^{*}P^{*}$	integrated daily primary production rates performed at light saturation	g C m^{-2} d^{-1}
$P_{max}(z)$	maximum photosynthetic rate at depth z	mg C m^{-3} h^{-1}
$\overline{P^{B}_{max}}$ [a]	mean, Chl-normalized $P_{max}(z)$	mg C mg Chl a^{-1} h^{-1}
$Q_{PAR}(z)$	photosynthetic available radiation at depth z	µmol quanta m^{-2} s^{-1}
$Q_{PAR}(0^{+})$	photosynthetic available radiation at the sea surface	µmol quanta m^{-2} s^{-1}
Ze	depth of 1% isolume (euphotic zone)	m
Zt	depth of the 0.1% isolume	m
Φ^{*} [a]	mean time-averaged quantum yield	dimensionless
Ψ	column light utilization index	g C (g Chl a^{-1}) m^2 (mol quanta)$^{-1}$
Ψ^{*}	column photosynthetic cross section	m^2 g Chl a^{-1}

[a] Unless explicitly specified in the text, the integrated or mean quantities refer to the layer between surface and Zt.

by trophic conditions). The variations in these input variables account for part of the variability of Ψ^{*} recorded in the field studies, with the remainder of this variability likely resulting from biological sources, namely from the photophysiological parameters typical of the algal assemblages [*Morel et al.*, 1996].

Reconciling empirical estimates of primary production with a mechanistic understanding of phytoplankton photophysiology has been the focus of many studies [e.g., *Platt*, 1986; *Campbell and O'Reilly*, 1988]. In particular, the biooptical model of *Morel* [1991] explicitly combines the P-I formulation and phytoplankton absorption properties to quantify Ψ^{*}. Using some simplifications, essentially Ψ^{*} can be expressed as

$$\Psi^{*} = \frac{\bar{a}^{*}\,\Phi^{*}}{4.6} \qquad (3)$$

where $\bar{a}^{*}$ is the spectrally averaged chlorophyll-specific absorption (g Chl a m^{-2}) and Φ^{*} (dimensionless) can be considered as a depth-time averaged quantum yield for photosynthesis, where carbon fixed and light absorbed have been both expressed in their energetic equivalent. The factor of 4.6 accounts for Ψ^{*} being calculated for the euphotic zone (from the surface to the depth where the radiant flux falls to 1% of its surface value. This factor is 6.9 if the layer considered extends to the depth of the 0.1% surface irradiance).

Analyzing the source of variability of the photophysiological parameters may therefore allow better understanding of the variability in the biogeochemical index Ψ^{*}. Quantum yield for photosynthesis and phytoplankton absorption are primarily light dependent [*Kiefer and Mitchell*, 1983]. Increasing evidence also suggests the dependency of these parameters upon the nutrient status [*Cleveland et al.*, 1989; *Marra and Bidigare*, 1994] or more generally upon the trophic status [*Wozniak et al.*, 1992; *Bricaud et al.*, 1995; *Babin et al.*, 1996], as well as upon algal pigmentation [*Bidigare et al.*, 1989; *Lindley et al.*, 1995; *Babin et al.*, 1996], temperature [*Tilzer et al.*, 1985; *Schofield et al.*, 1993], and differently ranked combinations of the above [*Schofield et al.*, 1993]. Given the recent documentation of the variability in these parameters, some of the discrepancies recorded in Ψ^{*} for historical data may be explained.

For the Southern Ocean, documentation of phytoplankton distribution, in situ rates of primary production, and associated photophysiological efficiency have been generally lacking. Therefore the accuracy of biooptical algorithms for prediction of Antarctic primary production on different timecales and space scales remains uncertain. The Southern Ocean has nevertheless received increasing attention in the context of the global change. Examples of this recent interest include : the capacity of those areas to respond to increasing anthropogenic CO_2 through biological sequestration [*Martin et al.*, 1990 a, b; *Mitchell et al.*, 1991] as well as the potential negative effect of UVB on carbon fixation in surface waters [e.g., *Smith et al.*, 1992; *Arrigo*, 1994]. Such topics clearly deserve to be investigated for the entire Southern Ocean using remote sensing and appropriate biooptical models to track phytoplankton productivity. In addition, present biooptical models are generally based on parameters derived from temperate or tropical latitudes. Therefore the problem of specific parametrization relevant to polar latitudes has to be addressed. Indeed, the seasonal sea-ice dynamics, the strong seasonality in incident irradiance, and the variability in wind- and density-induced upper ocean mixing are unique to polar environments and are recognized as determinant forcing variables of phytoplankton dynamics [*Whitaker*, 1982; *Rivkin and Putt*, 1988; *Moline and Prézelin*, 1996a].

As part of the Palmer Long Term Ecological Research (LTER) program [*Ross and Quentin*, 1992; *Smith et al.*, 1996a], a large database of primary production, algal pigmentation, and incident irradiance was acquired over a 3-year period (1991-1994) from late to early winter for a coastal Antarctic region. Even though the sampling stations were in shallow water, analyses shows that case I water predominated for most of the samples collected and enabled us to make comparisons relevant to the high-nutrient, often low-biomass waters of the Southern Ocean. Using this highly resolved data set, the column photosynthetic cross section has been derived

for 151 sample dates and the sources of variability have been assessed as a function of season and cloudiness, as well as phytoplankton biomass, photophysiology, and taxonomic dominance.

Materials and Methods

Sampling

During the austral spring/summer seasons of 1991-1994, intensive vertical profiling of physical, optical, biological, and chemical parameters related to phytoplankton dynamics was carried out at two coastal stations (B and E) within the nearshore grid of the Palmer Long Term Ecological Research program [*Waters and Smith,* 1992] (Figure 1). To date, this is the highest temporally resolved database for the Southern Ocean. It represents a sampling frequency of once every 4.5 days over a 3-year interval, with 151 vertical profiles collected for determination of primary production and associated photosynthetic parameters. For details of the depth/time distribution of discrete samples, see *Moline and Prézelin* [1996b]. Sampling was conducted from a Mark V Zodiac® with an effort to sample near solar noon. Whole water samples were collected in cleaned 5-L GoFlo® bottles, transferred to acid-washed dark bottles, and returned to Palmer Station within 30 min, where samples were stored in a cold room (-2 °C) until analysis.

Surface and In-Water Q_{PAR}

During the 1991-1992 season, measurements of surface and in-water Q_{PAR} were made using a Biospherical Instruments® scalar irradiance meter (QSR-170DT) equipped with a QSR-240 reference sensor. For the 1992-1993 and 1993-1994 seasons, Q_{PAR} measurements were performed using a Li-Cor® LI-193SA underwater quantum scalar irradiance sensor, a LI-190SA reference sensor, and a LI-1000 data logger. In addition to irradiance profiles taken during sampling, incident irradiance ($Q_{PAR}(0^+)$) was recorded continuously every 5 min over the three-year period at nearby Palmer Station. A comparison between data collected from the sensors at Palmer Station and data collected from the Zodiac® sampling platform showed that $Q_{PAR}(0^+)$ readings agreed to within 5%. Intercalibration of the reference sensors between years showed a difference of < 1%. Additionally, surface irradiance for clear-sky conditions was computed (D. Antoine, personal communication, 1996) according to *Morel* [1991] using standard conditions (350 Dobson units for ozone content, 2-cm precipitable water content, marine aerosol, and visibility of 23 km). Conversion from light energy to quanta was performed using a factor described by *Morel and Smith* [1974] for aquatic environments (2.5×10^{18} quanta per joule). From the in-water light field data, percent light depths expressed as the fractional ratio of $Q_{PAR}(z)$ to $Q_{PAR}(0^+)$ were determined for the sampling depths and then interpolated (linear interpolation of log-transformed data) vertically in the water column over 1-m intervals for use in estimates of in situ primary production rates resolved to the same vertical scale (see below). Percent light depths were assumed to be constant over the course of a single day. Transmission of $Q_{PAR}(0^+)$ through ice was held constant at 10%.

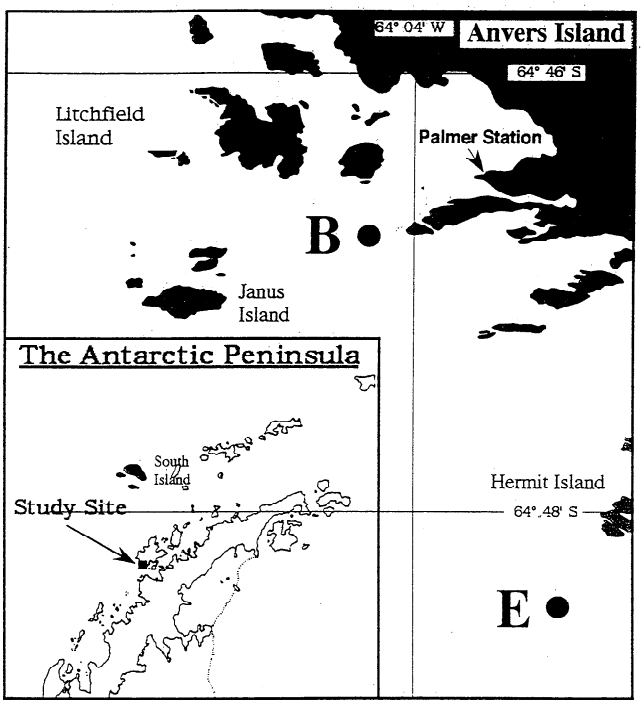

Figure 1. Location of the Palmer sampling stations B and E.

Pigments

The methods of extraction, analyses, and quantification, based on work by *Bidigare et al.* [1989] and *Wright et al.* [1991], have been carefully described by *Moline and Prézelin* [1996a]. In this study, algal pigments were used as taxonomic markers as follows: Chlorophyll *b* (Chl *b*) was the marker for green algae [*Jeffrey,* 1976], alloxanthin (Allo) for cryptophytes [*Gieskes and Kraay,* 1983], fucoxanthin (Fuco) for diatoms [*Wright and Jeffrey,* 1987], and the sum of 19'-hexanoyl-oxyfucoxanthin (Hex) and 19'-butanoyloxyfucoxanthin (But) for chromophytes-nanoflagellates (including *Phaeocystis pouchetii*). Although some species of *Phaeocytis* may contain significant amount of fucoxanthin [*Buma et al.*, 1991], there is evidence that this contribution remains low for Antarctic strains [*Vaulot et al.*, 1994; *Wright and Jeffrey,* 1987], especially in the Palmer area investigated here [*Bidigare et al.*, 1996]. The possible contribution of *Phaeocystis* to the fucoxanthin signal is therefore assumed to be negligible. In order to estimate the respective contribution of each taxonomic group, multiple-regression analyses were performed on vertically-integrated taxonomic pigment concentrations (surface to the depth of the 0.1% $Q_{PAR}(0^+)$ light level) against chlorophyll *a* [*Gieskes et al.*, 1988; *Bustillos-Guzman et al.*, 1995]. The regression analyses, performed on the data of each seasons gave the following results:

1991-1992

$$\text{Chl } a = 2.00\ \text{Fuco} + 3.15\ \text{Allo} + 1.99\ (\text{Hex} + \text{But}) + 0.68\ \text{Chl } b \quad (r^2 = 0.99,\ p<0.001)$$

1992-1993

$$\text{Chl } a = 1.54\ \text{Fuco} + 2.92\ \text{Allo} + 1.91\ (\text{Hex} + \text{But}) + 0.42\ \text{Chl } b \quad (r^2 = 0.94,\ p<0.001)$$

1993-1994

$$\text{Chl } a = 1.30\ \text{Fuco} + 3.49\ \text{Allo} + 1.45\ (\text{Hex} + \text{But}) + 0.50\ \text{Chl } b \quad (r^2 = 0.71,\ p<0.001)$$

For each sampling date, the chlorophyll *a* associated with each taxonomic group (diatoms, cryptophytes, nanoflagellates, green algae) was computed, using the above regressions, from

the concentration of its representative pigment (or group of pigments). Computed taxon-specific chlorophyll *a* concentrations were in turn used to estimate the contribution of each taxonomic group to the total biomass.

Primary Production

Primary production rates for this study were derived from photosynthesis-irradiance (P-I) relationships calculated for each of 756 discrete water samples. The procedures for incubation experimental design, sample handling, and calculation of photosynthetic parameters, as detailed for the 1991-1992 season by *Moline and Prézelin* [1996a], were the same used for the 3-year study. These procedures have been shown elsewhere to be largely free of any inhibitory effect induced by exposure to environmental ultraviolet radiation [*Boucher and Prézelin*, 1996]. The following photosynthetic parameters were derived by curve-fitting the equation described by *Neale and Richerson* [1987] (See (5) below; incubator light is substituted for the in situ light field) to experimental P-I measurements: P_{max} (mg C m^{-3} h^{-1}), the light saturated photosynthetic potential, I_k (µmol quanta m^{-2} s^{-1}), an estimate of the minimum irradiance required to saturate photosynthesis, α (P_{max}/I_k, (mg C m^{-3} h^{-1}) (µmol quanta $m^{-2}s^{-1})^{-1}$), the light-limited photosynthetic efficiency, β ((mg C m^{-3} h^{-1}) (µmol quanta $m^{-2}s^{-1}$) $^{-1}$), the efficiency of photoinhibition, and I_t (mmol quanta m^{-2} s^{-1}), the irradiance threshold for the onset of photoinhibition. Standard deviation estimates for the P-I parameters were calculated using the procedures described by *Zimmerman et al.* [1987]. Discrete P-I relationships with estimated standard deviations greater than 25% for P_{max} and/or 30 % for α were eliminated from this study.

Each of the P-I parameters were linearly interpolated at 1-m depth intervals between measurement depths and combined with estimated $Q_{PAR}(z)$ for each interval (see above) to calculate primary production. We believe interpolating light data and photosynthetic parameters over small depth intervals (1 m) will produce more accurate estimate of primary production than simply using trapezoidal integration between the depths at which P-I parameters were measured. Trapezoidal integration assumes a linear change of the integrated parameter between two consecutive depths. This assumption is reasonable for biological properties (i.e., photosynthetic parameters). However, this is not suitable to describe the exponential decrease in irradiance with depth. Therefore integrating primary production (as derived from the P-I formulation) over large depth intervals (5-10 m in this study) may lead to significant overestimation of production. In order to avoid this potential error, we calculated primary production at meter intervals and then integrated over depth. In situ primary production for each meter at 2-hour intervals over the day (P (z, t)) was calculated as a hyperbolic tangent [*Neale and Richerson*, 1987]:

$$P(z,t) = P_{max}(z)\tanh\left[\frac{Q_{PAR}(z,t)}{I_k(z)}\right] \quad (4)$$

when $Q_{PAR}(z, t)$ the measured integrated in situ irradiance for each 2-hour interval, was less than I_t (z) and

$$P(z,t) = P_{max}(z)\tanh\left[\frac{Q_{PAR}(z,t)}{I_k(z)}\right] \times \exp\{-\beta[Q_{PAR}(z,t) - I_t(z)] \quad (5)$$

when $Q_{PAR}(z, t)$ was greater than $I_t(z)$. It was assumed that P-I parameters remained constant over the day. The daily production rate was computed as the sum of the 12 daily 2-hour intervals.

For each depth/time interval, the production performed at light-saturation ($*P(z, t)$) was defined as follows : when $Q_{PAR}(z, t)$ was greater than $I_k(z)$, then $*P(z, t)$ was equal to the computed production $P(z , t)$ and when $Q_{PAR}(z, t)$ was less than $I_k(z)$, $*P(z, t)$ was assigned to be 0. Similarly, $*P(z, t)$ was integrated over time and depth to estimate daily integrated saturated production ($*P$). The ratio $*P/P$ therefore estimates the portion of the integrated production which occurs under light-saturated conditions.

The depth used for the integration of primary production and chlorophyll *a* significantly influences the value of Ψ^* (see (2)) [*Campbell and O'Reilly*, 1988; *Morel*, 1991]. For this study, all the Ψ^* values were calculated by integrating the chlorophyll content and primary production rates down to the 0.1% $Q_{PAR}(0^+)$ isolume. When the depth of this isolume was greater than the depth of the water column (< 3 % of the profiles), the data were integrated down to the maximum depths available (70 m for station B, 100 m for station E).

When computing Ψ^* using (2), Q_{PAR} appears both implicitly in the numerator, through the calculation of P, (see (4) and (5)) and explicitly ($Q_{PAR}(0^+)$) in the denominator. Therefore production and light are not independent variables in a statistical sense. Nevertheless, comparison between simulated in situ-based and P-I-based primary production estimates has been shown to be identical for this particular study site [*Boucher and Prézelin*, 1996]. This result is reassuring in estimating Ψ^* using P-I-based primary production estimate. It remains clear, however, that using the P-I technique is the most efficient method to generate highly resolved spatial and temporal primary production databases. The high number of samples collected is particularly important in the frame of this study since our goal is to examine the sources of variability in Ψ^*.

Results

Input Data for Ψ^* Calculations

The sampling days in this study incorporate the wide range of seasonal light changes characteristic for polar seas (Figure 2). Low daily irradiances (< 15 mol quanta m^{-2} d^{-1}) commonly

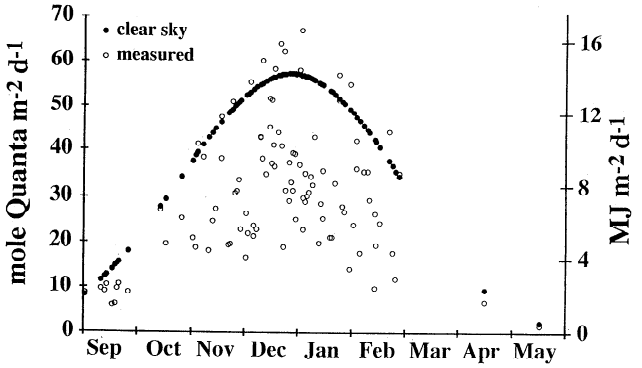

Figure 2. Temporal variations in surface irradiance at Palmer stations B and E, Antarctica. Each point represents a day where at least one sampling has been performed over the 3-year investigation at station B and/or Station E. For the purpose of convenience, units are expressed both in E m^{-2} d^{-1} and in MJ m^{-2} d^{-1}. Clear-sky irradiance computation is described in the "Material and Methods section".

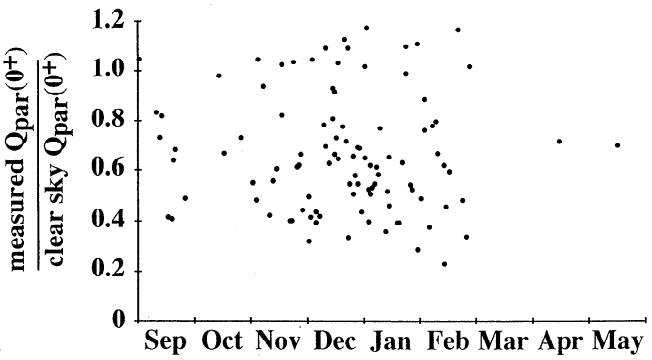

Figure 3. Temporal variation in cloud transmittance at Palmer stations B and E, Antarctica. Cloud transmittance is computed as the ratio between measured and clear-sky surface irradiance.

occurred during late winter (September) and fall (April-May) where day lengths were <6 hours long and midday solar zenith angle was >65°. Clear-sky daily integrated irradiance was fourfold higher at summer solstice when day length at the study site was approximately 20 hours and midday solar zenith angles was 40°. Measured daily irradiances during midsummer were occasionally higher than that modeled for clear-sky conditions (Figure 2), probably resulting from light reflectance off surrounding glacial ice and snow in this coastal environment. The effect of clouds on incident surface irradiance, quantified as the ratio of measured to clear-sky daily integrated $Q_{PAR}(0^+)$, was found to be seasonally independent (Figure 3). Cloudiness caused up to a fivefold variation in daily $Q_{PAR}(0^+)$.

Figure 4 summarizes the seasonal and interannual variation in water column phytoplankton biomass, primary production, and community composition for LTER station B during the 1991-1994 field seasons. The temporal dynamics for LTER station E were found to mimic those for Station B, with the details of the physical processes and the nutrient dynamics underlying these seasonal changes summarized by *Moline and Prézelin* [1996 a, b]. The 1991-1992 season was highlighted by a large month-long bloom (maximum 363 mg Chl *a* m^{-2}) responsible for high rates of in situ productivity (7.3 g C m^{-2} d^{-1}), followed by a 6-week period of low productivity. This pattern in biomass and productivity was not repeated in subsequent years where lower biomass (60 and 68 mg Chl *a* m^{-2} for the 1992-1993 and the 1993-1994 seasons, respectively) and productivity maximum (1.9 and 1.1 g C m^{-2} d^{-1}, for the 1992-1993 and the 1993-1994 seasons, respectively) were recorded during spring-early summer (note change of scales in Figure 4 for the 1992-1993 and 1993-1994 seasons). Despite this interannual variation in phytoplankton biomass and primary production, a quite reproducible annual pattern was recorded for the temporal evolution of the phytoplankton community structure (Figure 4). For the three seasons investigated, diatoms were always the dominant community for late spring/early summer with a transition to a cryptophyte-dominated communities in mid to late summer. Late winter conditions (as investigated for the 1993-1994 season) or fall conditions (as investigated for the 1992-1993 season) were characterized by an equal dominance of diatoms and nanoflagellates (Figure 4). Green algae were present at only a background level throughout the whole study (Figure 4).

The variable presence of terrigenous particles (including glacial flour in the Antarctic) and dissolved organic carbon (DOC) can alter optical properties of Antarctic waters in general [*Mitchell and Holm-Hansen,* 1991], including our study site [*Moline and Prézelin,* 1996a]. As a consequence, the amount of light available for photosynthesis may be reduced and thereby may be a potential source of influence on Ψ*. We employed the relationship from *Morel* [1988] to discriminate between case I (those where phytoplankton and their derivatives play a dominant role in determining optical properties) and case II (where the optical properties are mainly governed by other substances than phytoplankton and their derivatives) waters in our present data set. Figure 5 shows the relationships between measured euphotic zone depth (*Ze*) and the corresponding mean $\overline{Chl}$ content in this layer. Of the total determinations, 75% of the observations were performed for typical case I waters. If profiles which were ice covered are removed, as ice may bias estimation of the light attenuation, then 80% of the profiles sampled were in case I waters. Therefore, despite the proximity to the coast, most of the observations were under little influence from terrigeneous material or DOC. Nevertheless, for 20 % of the profiles, attenuating particles other than phytoplankton biomass may have influenced water optical properties and thereby potentially primary production and resulting estimates of Ψ*.

Estimation of Ψ*

For the entire data set, 85% of the variance recorded in primary production was explained by the product of <Chl> and $Q_{PAR}(0^+)$ (Figure 6). The regression line has a negligible intercept and a slope (which is an estimate of Ψ*) of 0.0695 m^2 g Chl a^{-1}. This value typically falls in the range of Ψ* estimates from various tropical and temperate open oceans [*Platt,* 1986; *Morel,* 1991] and is close to the values reported by *Prasad et al.* [1995] for coastal waters of the Gulf of Mexico.

The frequency distribution of Ψ* was found to be nonnormally distributed, with a median of 0.088 m^2 g Chl a^{-1} and an average of 0.109 m^2 g Chl a^{-1} ± 0.075 (Figure 7). This average value corresponds to what is considered as an upper limit for Ψ* [*Platt,* 1986; *Morel,* 1991]. The range of variation at 1 standard deviation extends over a factor of 5.4 (compared to threefold for temperate and tropical area) and the extreme values recorded in this studies extend over a fiftyfold range (0.009-0.488 m^2 g Chl a^{-1}). The sources of this high variability in Ψ*, which seems to be a particular feature of this region, will now be further detailed.

Sources of Variability in Ψ*

Results focus on two kinds of variables; those which are explicit in the formulation of Ψ* in (2) (e.g., <Chl>, $Q_{PAR}(0^+)$) and those which are implicit in this formulation and affect the rates of primary production (i.e., the taxonomic composition (and associated absorption and efficiency properties) and the in-water light field (as influenced by pigments and/or other substances)). The problem in identifying (and quantifying) sources of variability is that (1) forcing variables occur simultaneously and (2) their effects are not simply additive but result from complex, nonlinear interactions. Therefore we will first focus on known sources of variability in Ψ* (surface irradiance, as affected by cloudiness and seasonality) and then selectively remove the influence of this variability before identifying other potential sources and their associated effects on Ψ*. This is the first time such a stepwise approach has been used on field data, and the only comparable results are those

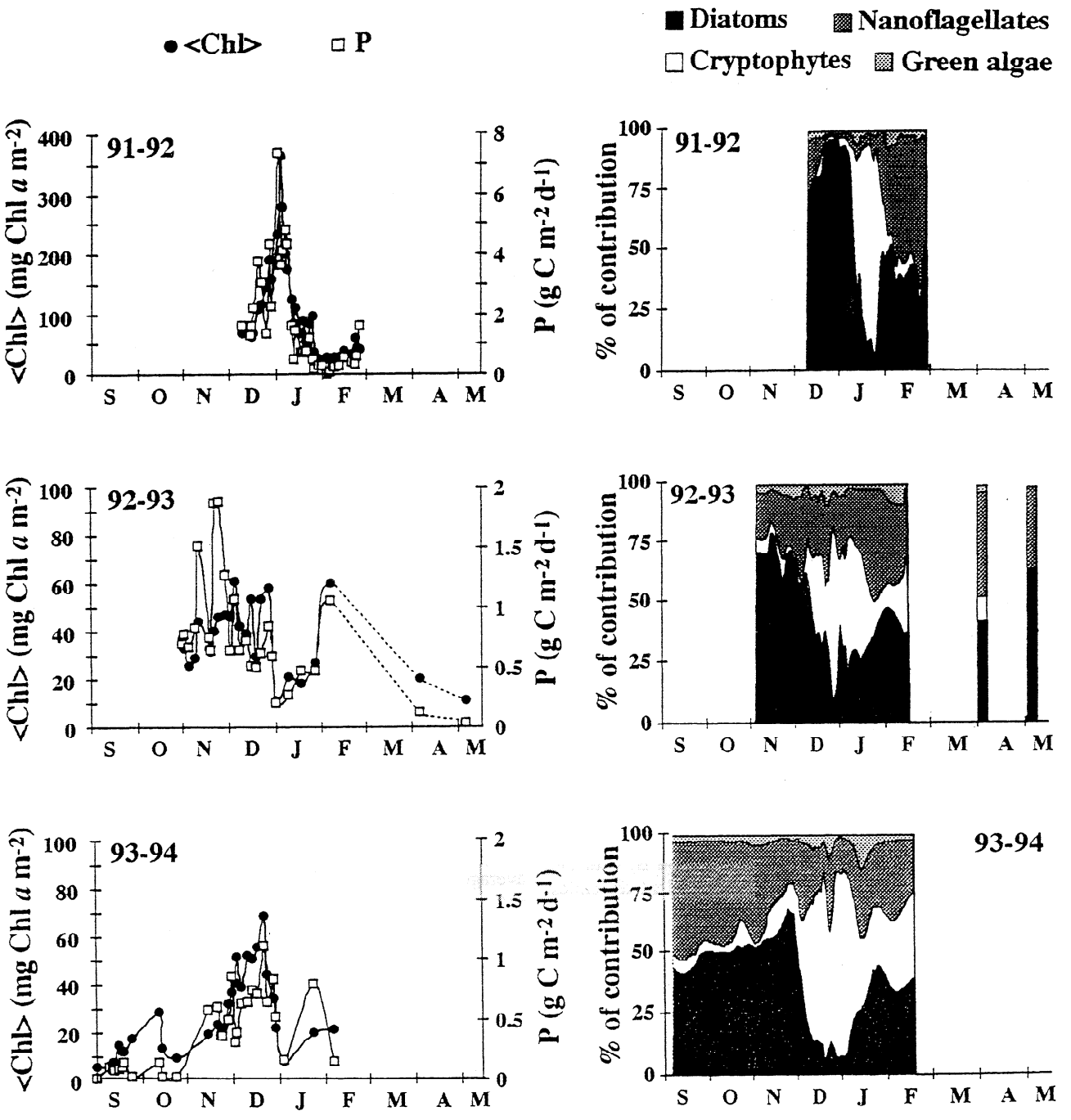

Figure 4. Temporal evolution of phytoplankton dynamics at Palmer station B, Antarctica. The left panels refer to phytoplankton biomass and primary production. The right panels refer to phytoplankton community structure.

modeled by *Morel* [1991] and the subsequent analysis performed by *Antoine and Morel* [1996].

Cloudiness. Cloud coverage was responsible for high day-to-day variations in the surface irradiance (see above and Figure 3). The reduction of incident irradiance by clouds had a positive effect on Ψ^* (Figure 8), confirming previous modeled results [*Morel*, 1991]. The clear nonlinear relationship between cloud transmittance and the ratio of measured Ψ^* to that calculated for clear-sky conditions are accurately described by an empirical powerlaw function ($r^2 = 0.77$, n=151, Figure 8). When the cloudiness effect is removed from the present data set (clear-sky conditions), this leads to a frequency distribution in Ψ^* (Figure 9) closer to a normal distribution than that which was observed using the measured light (Figure 7). The median is equal to 0.071 m^2 g Chl a^{-1} and the average 0.090 m^2 g Chl $a^{-1} \pm 0.070$) and the range of variation at 1 standard deviation extends over a range of about 8. Large variability in Ψ^* still persists when cloud cover is eliminated.

Seasonality in incident irradiance. An apparent seasonal pattern in Ψ^* (computed for clear-sky conditions) was recorded during this study (Figure 10). High values were associated with late and early winter conditions, while the lowest values were associated with the months surrounding the austral summer solstice. The minimum of the empirical polyno-

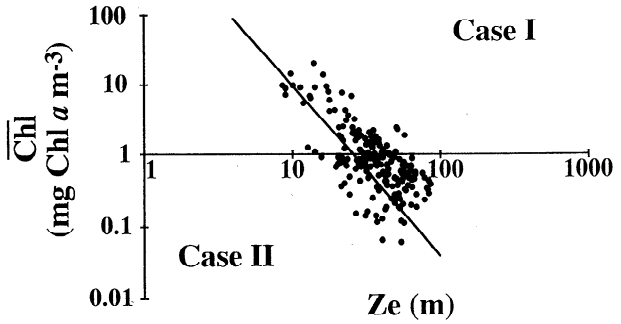

Figure 5. Optical type of waters at Palmer station B and E, Antarctica. Plot of $\overline{Chl}$ within the euphotic layer (*Ze*) versus the depth of this layer. The equation of the line is $Y = -2.40X + 3.40$ (with $Y = \log_{10}(\overline{Chl})$ and $X = \log_{10}(Ze)$) and was given by *Morel* [1988] as a criteria to differentiate between case I waters (right side of the line) and case II waters (left side of the line).

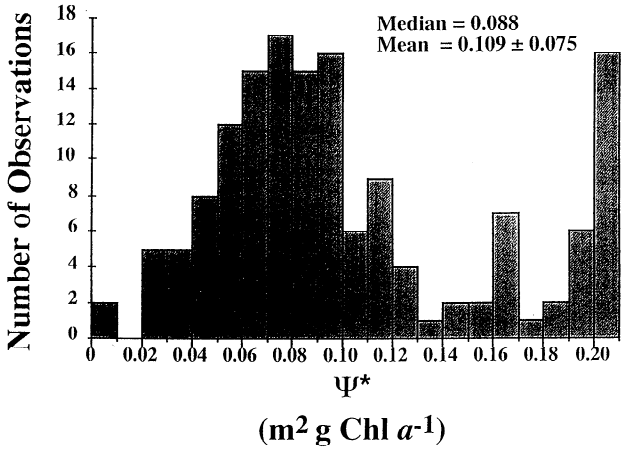

Figure 7. Frequency distribution of Ψ* for the whole data set. Ψ* is computed using irradiance measurements.

mial function fitted to the data occurs 2 weeks after the maximum surface irradiance (Figure 2). Part of this delayed response may reveal a critical timescale between the actual seasonal light forcing and the effective change in the biogeochemical status of the water column through adaptation processes (from physiological adaptation to species changes). In fact, these two weeks have been identified as a critical timescale for quantitative and qualitative phytoplankton changes in this highly dynamic region [*Moline and Prézelin*, 1996a].

The range of variation in Ψ* for the entire data set (as estimated from the empirical polynomial function reported in Figure 10) varies over sixfold, which confirms previous modeled results [*Morel*, 1991], and illustrates the importance of seasonal changes for high-latitude regions. Additionally, this sixfold range can be considered as a lower limit since the highest values, associated with ice conditions, are minimal estimates because light transmission through ice was often lower than the 10% used here. To our knowledge, the only other study attempting to highlight potential seasonal changes in column photosynthetic cross section on the basis of field measurements was by *Campbell and O'Reilly* [1988]. No clear seasonal relationships appear in their data and this likely results from the latitude of the study (along the northwestern Atlantic continental shelf, 36°-44°N), where the range of seasonal variation in surface irradiance (less than threefold) is lower than in the present investigation (more than sevenfold).

If the data set is restricted to a period of 2 months centered around the summer solstice (removing seasonal effect) (November 21 to January 21), the frequency distribution of Ψ* (for clear-sky condition) is near normal, where the median (0.060 m^2 g Chl a^{-1}) nearly equals the average (0.064 m^2 g Chl a^{-1} ± 0.027) (Figure 11). The range of variation at 1 standard deviation is now 2.5, which is below the range reported for a compilation of data from various provinces [e.g., *Platt*, 1986]. It is interesting to note that the model of *Morel* [1991], using standard parameters for characterizing phytoplankton photophysiology, adequately reproduces the mean value recorded in the field as well as explains a great part of the variability. The principal determinant source of variability in this model is linked to the surface irradiance variation as driven by seasonality and cloudiness, while trophic status as characterized by chlorophyll concentration has little impact on the recorded variability [*Morel*, 1991] (see later). Even with the seasonality and cloudiness removed, significant variability still exists in Ψ* (Figure 11). This variability is likely due to biology and to the possible variations in phytoplankton photophysiology.

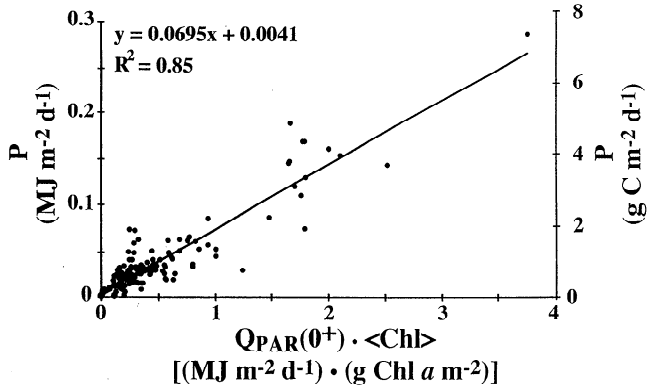

Figure 6. Estimation of the column photosynthetic cross section for the whole data set. The slope of the regression *P* versus $Q_{PAR}(0^+)$ times <Chl> gives estimate of Ψ*. For the purpose of convenience, primary production is expressed either in MJ m^{-2} d^{-1} or in g C m^{-2} d^{-1}.

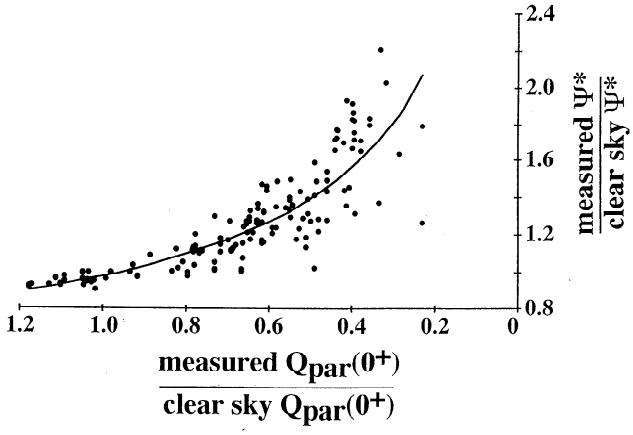

Figure 8. Effect of cloud transmittance on Ψ*. Cloud transmittance is computed as the ratio between measured and clear-sky surface irradiance. The ordinate presents the ratio of Ψ* computed for measured surface irradiances divided by Ψ* computed for clear-sky surface irradiances (see also Figure 3).

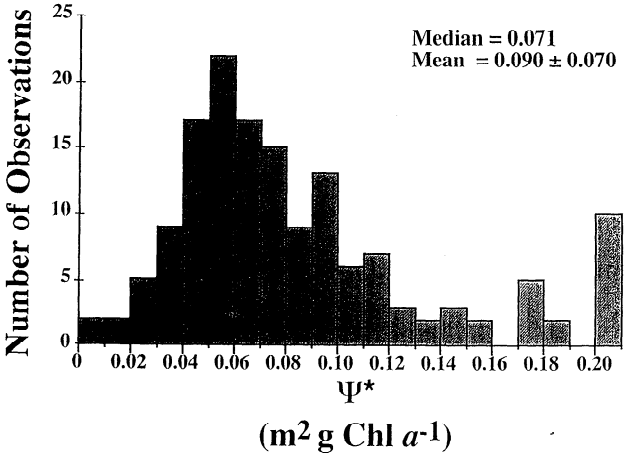

Figure 9. Frequency distribution of Ψ*, when computed for clear-sky conditions and for the whole data set.

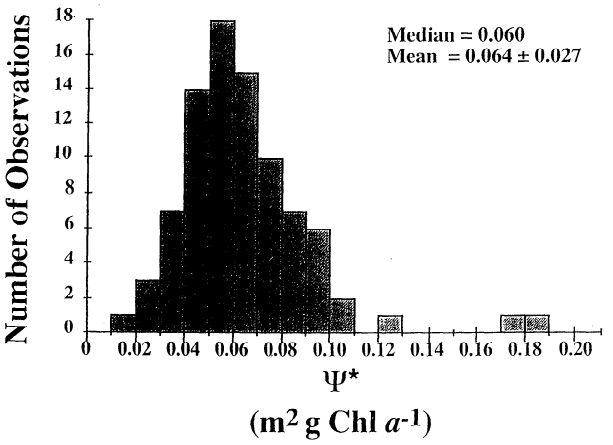

Figure 11. Frequency distribution of Ψ* for the period November 21 to January 21. Ψ* is computed for clear-sky conditions.

Chlorophyll *a* concentration. The large range of chlorophyll concentration over the 3 years (average water column chlorophyll from 0.11 to 19.08 mg Chl *a* m^{-3}) provides an opportunity to test a potential biomass effect on Ψ*. In order to reduce any influence from other sources of variability, here we consider only the Ψ* data computed for clear-sky conditions (removal of cloud effect, Figure 8) for the 2-month period around the summer solstice (removal of the seasonal effect, Figures 2 and 10). We further restricted the data set to quasi-monospecific populations to minimize group-specific effects on Ψ*, which will be shown later to be significant. Data were partitioned according to a $\overline{Chl}$ threshold of 2 mg Chl *a* m^{-3}. For diatom-dominated communities, when $\overline{Chl}$ increased of a factor 7 (from 1.1 to 7.3 mg Chl *a* m^{-3}), Ψ* decreased by a factor 1.7 (*t*-test, $p < 0.02$) (Table 2). Such a reduction in Ψ* associated with increasing chlorophyll biomass is higher than expected from modeled results [*Morel*, 1991], which predict a reduction in Ψ* of only approximately 10 % for the same biomass range. For cryptophyte-dominated communities, the range of chlorophyll concentration investigated here is only 3 (from 1.3 to 3.8 mg Chl *a* m^{-3}) and a associated reduction of a factor 1.5 (*t*-test, $p < 0.02$) is also observed (Table 2).

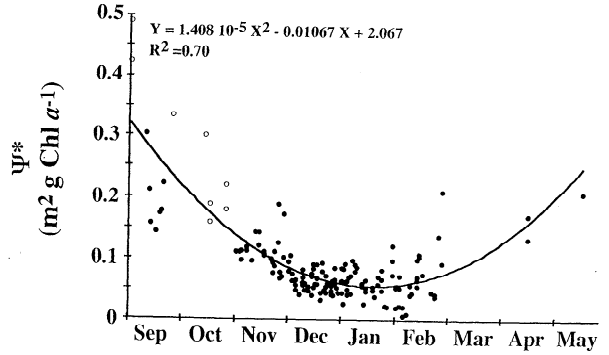

Figure 10. Seasonal variations in Ψ*. In order to remove any short-term effects of surface irradiance changes induced by cloud attenuation (see Figures 3 and 8), Ψ* was computed for clear-sky conditions. In the polynomial function fitted to the data, *X* corresponds to Julian day (where January 1 is equal to day 366 and so on for the following days). Open circles indicate ice-covered waters; solid circles indicate ice-free waters.

Phytoplankton community structure. Because of taxon-specific physiological differences, species dominance and succession can be viewed as an adaptation to changing environmental conditions. One may consequently wonder if the column photosynthetic cross section is dependent on the dominant taxon. Such a taxonomic dependency on Ψ* was mentioned by *Balch and Byrne* [1994] as a possible explanation for the recorded regional variations. Table 2 presents the average values of Ψ* for various, single taxon-dominated phytoplankton communities. Considering all profiles (except those ice covered) where a single taxon contributes to more than 50% of the chlorophyll biomass, Ψ* for diatoms was greater than that for cryptophyte by 77% (*t*-test, $p < 0.001$) and greater than that for nanoflagellates by 60% (*t*-test, $p < 0.02$).

Table 2. Influence of Chlorophyll Concentration and Phytoplankton Community Structure on Ψ* at Palmer Stations B and E, Antarctica

Taxonomic Group	Ψ* [a]	*n*
Taxonomic Group Contribution >70% of <Chl> [b]		
Diatoms [c]	0.114 ± 0.051	6
Cryptophytes [c]	0.053 ± 0.011	13
Diatoms [d]	0.068 ± 0.020	14
Cryptophytes [d]	0.034 ± 0.013	3
Taxonomic Group Contribution >50% of <Chl>		
Diatoms	0.094 ± 0.041	50
Cryptophytes	0.053 ± 0.017	31
Flagellates	0.059 ± 0.035	16

When the contribution by each taxonomic group is > 70% of <Chl>, the data set is divided according to a mean chlorophyll concentration threshold of 2 mg Chl *a* m^{-3}. A subset of Ψ* is further presented, where each phytoplankton group accounts for > 50% of <Chl>. Values are reported as the mean ± 1 standard deviation.

[a] For clear-sky conditions only, in order to remove any potential cloud effect on Ψ* (see text and Figure 6).

[b] For November 21 to January 21 of any given year 1991-1994: this date restriction prevents any effect of seasonal incident irradiance change on Ψ* (see text and Figure 10).

[c] $\overline{Chl}$ < 2 mg Chl *a* m^{-3}

[d] $\overline{Chl}$ > 2 mg Chl *a* m^{-3}

But such comparisons suffer from the possible interference of seasonality in surface light or from some biomass effect (see above). Therefore the data set was again restricted to the period around the summer solstice (November 21 to January 21), and the samples were partitioned according to a $\overline{Chl}$ threshold of 2 mg Chl a m^{-3} (Table 2). In order to deal with quasi-monospecific populations, only those data where a single taxonomic group contributes to more than 70% of the chlorophyll biomass were considered. Using such restrictions, the data set is limited; however, it clearly shows that Ψ^* for diatoms was 2.15 times higher than for cryptophytes ($p < 0.001$) when $\overline{Chl}$ was lower than 2 mg Chl a m^{-3} and 2 times higher when $\overline{Chl}$ was greater than 2 mg Chl a m^{-3}. Therefore we can conclude that for the same amount of chlorophyll in the water column and for the same incident irradiance, daily integrated primary production is depressed by a factor of 2 when cryptophytes replace diatoms.

Discussion

The Southern Ocean is a particularly challenging environment for which it is a tedious task to acquire in-water data sets capable of adequately resolving the temporal variability in primary production on interannual, seasonal, and subseasonal timescales. The difficulties arise, in part, to the remoteness of the study sites, the extreme working conditions, and the labor-intensive aspects of making simultaneous measurements of primary production and the associated environmental variables which may influence rates of in situ carbon fixation. The rationale for acquiring such data sets, like that employed in the present analysis, is to provide means to test remote-sensing algorithms which have been developed using ground truth data from other latitudes and thereby extend the ability to make temporal and spatial estimates for primary production in the Southern Ocean. Satellite imagery has provided chlorophyll biomass maps which detect the presence and distribution of episodic phytoplankton blooms in various regions of the Southern Ocean [*Comiso et al.*, 1993; *Sullivan et al.*, 1993; *Arrigo and McClain*, 1994]. For waters west of Palmer Peninsula, where the Palmer Long Term Ecological Research Program has maintained a mesoscale grid of sampling stations since 1990 [*Waters and Smith*, 1992], patterns of chlorophyll distribution measured during the offshore LTER, Icecolors cruises [*Prézelin et al.*, 1992; *Bidigare et al.*, 1996; *Smith et al.*, 1996a] agree well with the historical (pre 1986) satellite imagery for the same region [*Smith et al.*, 1996b]. Converting such chlorophyll maps into primary production maps requires the knowledge of the efficiency at which incident irradiance is utilized to drive marine photosynthesis and thereby convert inorganic carbon into stored, chemical energy.

Predicting Primary Production From Chlorophyll and Surface Light Fields

The results of our analyses of the LTER coastal data set for 1991-1994 clearly show that the product of incident irradiance and the integrated chlorophyll content is a good predictor of integrated daily primary production rates, as it explains 85% of the recorded variance (Figure 6). To date, there have been few attempts to determine the column photosynthetic cross section in polar areas. Until now, the work by *Holm-Hansen* and *Mitchell* [1991], as part of the Racer Program in a nearby region of coastal waters, has been the only study to provide estimates for Antarctic waters ($\Psi^* = 0.050 \pm 0.022$ m^2 g Chl a^{-1}, n=18). Other estimates of Ψ^* for high latitudes were provided by *Yoder et al.* [1985] for Canadian Arctic (0.091 m^2 g Chl a^{-1}) and Sub-Arctic Pacific (0.049 m^2 g Chl a^{-1}). The values of Ψ^* determined by the regression line in Figure 6 ($\Psi^* =$ 0.0695 m^2 g Chl a^{-1}) are equal to what is generally considered as standard for temperate and/or tropical areas [*Morel*, 1978; *Platt*, 1986]. Therefore the standard value of 0.07 m^2 g Chl a^{-1} appears to be accurate for first-order mapping of production rates from synoptic estimates of chlorophyll biomass and from incident irradiance for this area. Moreover, we demonstrate (Figure 5) that most of the sampling stations (75%) were typical of case I waters (this contribution was even greater (80%) if sampling date with ice was removed). Therefore, although the present data set was collected from nearshore stations, our conclusions may also be considered relevant to open ocean waters of the Southern Ocean.

The close agreement between estimates for Ψ^* in warmer waters and the Palmer region suggests that the temperature effect on Ψ^* is minimal; this, however, is still a matter of controversy. While *Tilzer et al.* [1985] and *Li* [1985] suggested that photosynthesis rates in polar phytoplankton are temperature limited, other results have shown otherwise [e.g., *Priddle et al.*, 1986]. Furthermore, it is accepted that respiration rates are more strongly affected than photosynthetic rates by depressed temperatures [*Tilzer and Dubinsky*, 1987]. Consequently, in polar regions, gross production is expected to be closer to net production than in tropical/temperate areas. Therefore the likelihood that our gross (because of short incubation time) production measurements approximate net (long incubation time) production increases the validity of comparing our Antarctic Ψ^* estimates with those from warmer latitudes where net primary production measurements generally dominate the data sets used for Ψ^* calculations.

Light-Saturated Versus Light-Limited Photosynthesis and Ψ^*

Studies attempting to link biooptical algorithms to the mechanistic understanding of primary production have emphasized the importance of I_k [*Platt*, 1986; *Platt and Sathyendranath*, 1993; *Morel et al.*, 1996], the irradiance level at which primary production begin to be saturated. Over this 3-year sampling period, almost 50% of the production was performed at saturation (Figures 12a and 12b), and this proportion is even higher when the data set is restricted to a period of 2 months encompassing the summer solstice (November 21, January 21 (Figures 12c and 12d). This finding has important consequences related to the reduction of irradiance, either incident (by clouds) or in-water (by other substances than phytoplankton in case II waters), and its effect on primary production and Ψ^* evaluation.

Consider a hypothetical case where production is exclusively light dependent (this means, at each time of the day and at each depth, production is performed on the light-limited portion of the P-I relationship). Any decrease in surface irradiance (i.e., cloud cover) would be reflected by a proportional decrease in the production (equation (4)) and therefore no change in Ψ^* (equation (2)). However, this was not seen in this study, and the strong nonlinear relationship observed between cloud transmittance and the ratio of Ψ^* for measured and clear-sky irradiance (Figure 8) is a direct consequence of the part of primary production lying outside the light-limited range (Figure 12). Due to the large variability of cloud transmittance on a daily scale (Figure 3), accurate estimation

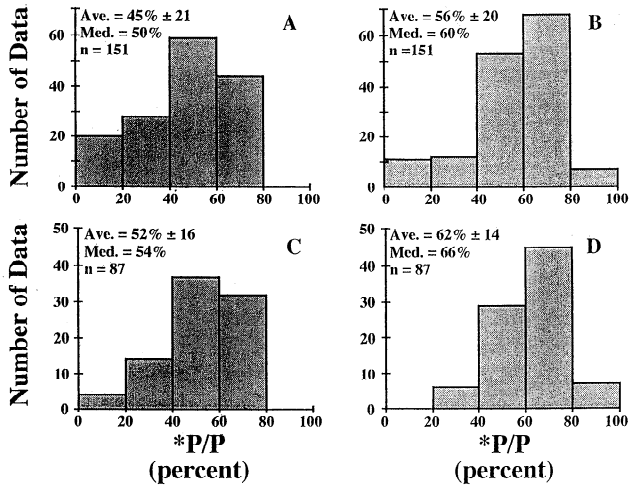

Figure 12. Frequency distribution for the portion of the daily integrated primary production performed under light saturation (P^*/P). (a) Whole data set, using measured irradiance. (b) Same as Figure 12a, but for clear-sky irradiance. (c) Data set restricted to November 21 to January 21, using measured irradiance. (d) Same as Figure 12c but for clear-sky irradiance.

of primary production from chlorophyll fields therefore requires precise knowledge of the incident irradiance.

In this hypothetical case of totally light-limited production, any reduction of the in-water light field by non-phytoplankton sources would result in a proportional reduction in primary production for the same surface irradiance and chlorophyll concentrations. Consequently, Ψ^* would be proportionally reduced. Because a large proportion of production was performed on the light-saturated range in the present study (Figure 12), we may expect a reduction of the in-water light field not to have a strong effect on Ψ^*. This possible influence of the water types on Ψ^* has never been addressed. To approach this problem, we first used the regression line (see Figure 5) given by *Morel* [1988] (discriminating between case I and case II waters) to calculate the chlorophyll content for each sampling date from the (known) euphotic zone depth. The measured chlorophyll content was then ratioed with this calculated quantity. The ratio was expected to be an index for the type of water, with ratio values lower than 1 characterizing case II waters (left side of the line on Figure 5), and values greater than 1 describing case I waters (right side of the line on Figure 5). As this index increased, the average values of Ψ^* (computed for clear-sky conditions and for the period around the summer solstice) increased slightly; however, the trend is not significant (Figure 13). This results not only from the high proportion of saturated production in the water column (Figure 12) but also from the fact that case II waters in this study were not strongly departing from case I waters, from an optical viewpoint. A more general conclusion from this result is that the use of Ψ^*-based approaches to estimate primary production can be extended from case I to some moderately turbid case II waters, as long as a significant portion of the production is performed at saturation.

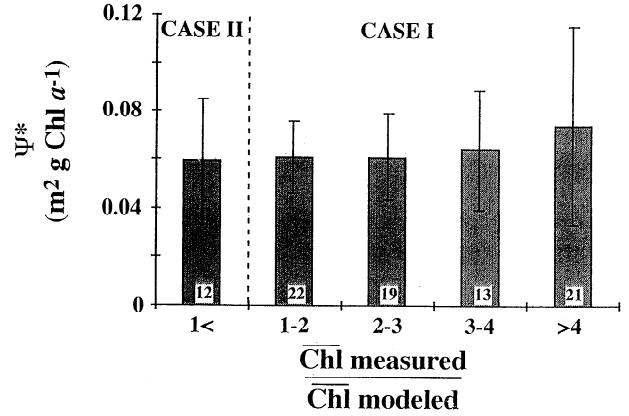

Figure 13. Independence of Ψ^* on the water optical types. The data set is restricted to the period November 21 to January 21 and Ψ^* is computed for clear-sky conditions. The insert numbers refer to the number of data points (also see text).

Ψ^* and Photophysiological Properties

Dependence of Ψ^* on α^B. On the basis of theoretical considerations, *Platt* [1986] argues that the light utilization index (see (1)) can be considered, as a first approximation, to be proportional to α^B, the chlorophyll *a*-normalized slope of the P-I relationship. The bias introduced by such an approximation depends on the fraction of primary production which is performed in the light-saturated range. Obviously, such a direct proportionality between α^B and Ψ^* is not expected within the present data set, given the large portion of production realized outside the range of light-limited photosynthesis (Figure 12). Despite this potential discrepancy, Ψ^* and $\bar{\alpha}^B$ (depth-averaged values of α^B are considered here for the purpose of simplification, assuming homogeneous distribution of this pa-

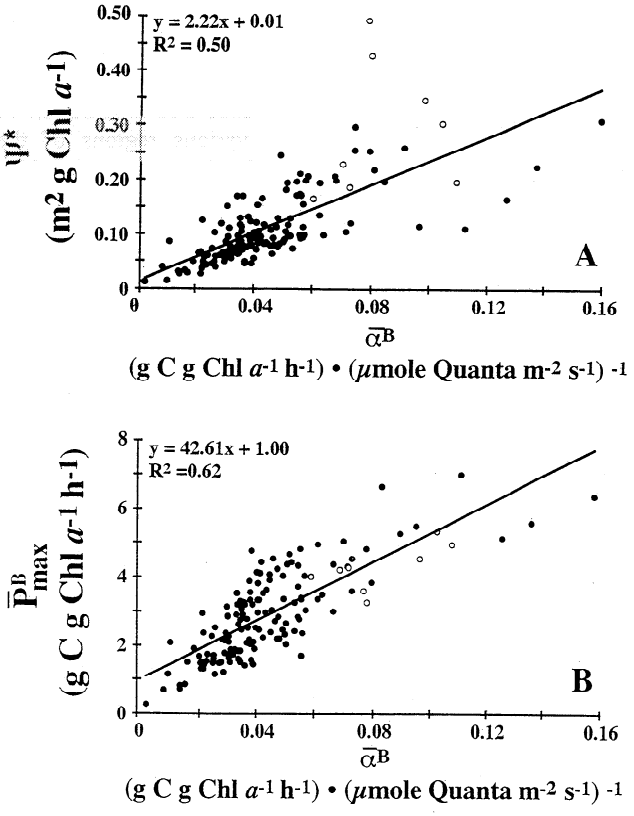

Figure 14. Ψ^* and photophysiological parameters at Palmer stations B and E, Antarctica: (a) Relationship between $\bar{\alpha}^B$ and Ψ^*. (b) relationship between $\bar{\alpha}^B$ and $\bar{P}^B_{max}$. Open circles indicate ice-covered waters; solid circles indicate ice-free waters.

rameter with depth) covary and at least 50% of the variability recorded in Ψ^* can be attributed to change in $\bar{\alpha}^B$ (Figure 14a). This significant relationship is largely the reflection of the strong covariation between P^B_{max} and $\bar{\alpha}^B$ (Figure 14b). Any increase in $\bar{\alpha}^B$ is associated with a proportional increase in P^B_{max} Consequently, for primary production evaluation, any increase of $\bar{\alpha}^B$ will be roughly followed by a proportional increase in production, whatever the portion (light-limited or light-saturated) of the P-I relationship production occurs. Another conclusion from Figure 14b is that the slope of the regression P^B_{max} versus $\bar{\alpha}^B$, if forced to be 0, provides a rough depth- and time-averaged value for I_k, 60 μmol quanta m^{-2} s^{-1}. Given that this estimation is derived from a linear regression based on averaged quantities, it does not reflect the possible depth or time dependent variations of I_k due to photoadaptation. Nevertheless, due to the significant covariation of both $\bar{\alpha}^B$ and P^B_{max}, this value of I_k can be considered as a standard input value for biooptical models which attempt to estimate primary production on large scales. Since I_k values are spectrally dependent parameters (and so depend on spectral output of the incubator lamps), direct comparison with other estimates are conditional. Nevertheless, the I_k values estimated here are in agreement with most values reported for Antarctic waters [*Smith and Sakshaug*, 1990, and references therein] and specifically for the Palmer region [*Smith et al.*, 1996b, and references therein].

Chlorophyll *a* range and Ψ^*. For typical diatom-dominated conditions, Ψ^* was depressed by a factor of 1.7 when chlorophyll concentration increased from 1.1 to 7.3 mg Chl *a* m^{-2} (Table 2). From (3), such variation in Ψ^* can be analyzed in term of the change in the absorption term ($\bar{a}^*$) and quantum yield (Φ^*). From in situ investigations, it has been shown that the maximum quantum yield for photosynthesis decreases with decreasing nutrient concentrations [e.g., *Cleveland et al.*, 1989; *Babin et al.*, 1996]. Since nitrate-replete conditions are a well-known feature of Antarctic waters, we can therefore argue that nitrate limitation, as possibly influenced by the trophic status (chlorophyll concentration), did not affect the maximum quantum yield. Moreover, the theoretical study of *Morel* [1991] emphasizes that Φ^* (which differs from the maximum quantum yield as it is an operational quantum yield) does not significantly change with chlorophyll concentrations ranging from 1 to 7 mg Chl *a* m^{-3}. In the present study, the reduction in Ψ^* associated with increasing biomass (Table 2) was not associated with a similar change in the average photosynthetic parameters (P^B_{max} decreases by 5% and $\bar{\alpha}^B$ by 16% (nonsignificant changes), Table 3). It seems therefore that the column photosynthetic cross section is depressed with increasing chlorophyll biomass, while photosynthetic performance remains nearly unchanged. We can reasonably suspect that most of the variation recorded in Ψ^* with increasing chlorophyll is therefore related to the absorption term $\bar{a}^*$. The estimation of true chlorophyll-specific absorption by phytoplankton was not evaluated as part of this study, and only a reconstructed unpackaged spectrum can be obtain from the pigment data (see below). Nevertheless, a recent synthetic analysis performed by *Bricaud et al.* [1995] emphasizes that chlorophyll-specific absorption decreases with increasing chlorophyll concentration and that this variation is likely due to (1) increasing of packaging and (2) decreasing of accessory pigmentation. *Bricaud et al.* [1995] demonstrated that, on average, chlorophyll-specific absorption by phytoplankton can be predicted from chlorophyll concentration using an empirical power law function. By using this proposed function, the computed specific absorption coefficient (here calculated at 440 nm) decreases by a factor of 1.87 for chlorophyll range from 1.1 to 7.3 mg Chl *a* m^{-3} (Table 3). Assuming that Φ^* was affected little by increasing chlorophyll concentration, we can conclude that a reduction in the overall specific absorption coefficient as a result of increasing packaging effect may account for most of the 70% reduction in Ψ^* associated with the biomass increase (Table 3).

Dominant taxa and Ψ^*. When diatoms were dominating the phytoplankton community, the water column was twice as efficient in converting solar energy into chemical energy as when cryptophytes were dominant (Table 2). Considering mean chlorophyll concentrations of about 1 mg Chl *a* m^{-3}, $\bar{\alpha}^B$ and P^B_{max} for cryptophytes were lower than $\bar{\alpha}^B$ and P^B_{max} for diatoms, by factors of 1.6 and 2.3, respectively (Table 3). For higher chlorophyll concentrations, this reduction was 1.8 and 3.1 for $\bar{\alpha}^B$ and P^B_{max}, respectively. These taxonomic differences in the photosynthetic parameters of both diatoms and cryptophytes (Table 3) may therefore explain most of the recorded variations in Ψ^* (Table 2). Pigmentation differences of both algal groups provide additional information. Cryptophytes contain phycobiliproteins [*Rowan*, 1989], providing a competitive advantage over diatoms for green-light harvesting (i.e., bloom conditions). The primary carotenoid of diatoms is the photosynthetic fucoxanthin, and for cryptophytes it is alloxanthin [*Rowan*, 1989], which is considered to be photoprotective [*Marra and Bidigare*, 1994]. The photoprotective function prevents a nonnegligible portion of absorbed light from being directed to reaction centers and used for photosynthesis. This proportion was estimated for both phytoplankton groups using the comparison of a spectrally averaged (pertinent to the incubator light field) chlorophyll-specific ab-

Table 3. Variations in Average Photophysiological Properties as a Function of Dominant Taxa and Mean Chlorophyll Concentration at Palmer Stations B and E, Antarctica

Taxonomic Group	$\overline{\text{Chl}}$ [a]	P^B_{max}	$\bar{\alpha}^B$	$\bar{a}^*$ [b]	$\bar{a}^*_{act}$ [b]	n
Diatoms	1.1 ± 0.4	3.9 ± 0.7	0.051 ± 0.019	9.99 ± 0.52	9.32 ± 0.44	6
Diatoms	7.3 ± 4.5	3.7 ± 0.9	0.043 ± 0.009	9.32 ± 0.24	8.89 ± 0.19	14
Cryptophytes	1.3 ± 0.4	1.7 ± 0.4	0.032 ± 0.007	7.32 ± 0.49	5.98 ± 0.26	13
Cryptophytes	3.8 ± 0.4	1.2 ± 0.3	0.024 ± 0.011	6.77 ± 0.32	5.46 ± 0.18	3

The data set is restricted to the period Nov 21 to Jan 21 of any given year 1991-1994, and only those samples where a taxonomic group contribution equals to > 70% of <Chl> are considered (see Table 2). Values are reported as the mean ± 1 standard deviation.

[a] Data are grouped according to a Chl threshold of 2 mg Chl *a* m^3 (see Table 2).

[b] Spectrally averaged absorption coefficients were derived from spectral reconstruction procedures [*Bidigare et al.*, 1990], using mean pigment concentrations.

sorption coefficient with ($\bar{a}^*$) and without ($\bar{a}^*_{act}$) the contribution of photoprotective pigments (Table 3). These coefficients are determined from reconstruction techniques based on the concentration of individual liposoluble pigments [*Bidigare et al.*, 1990]. A comparison of $\bar{a}^*$ or $\bar{a}^*_{act}$ for diatoms and cryptophytes is not strictly relevant here since the absorption contributions of cryptophyte hydrosoluble phycobiliproteins, not quantified in this study, are not taken into consideration (therefore the coefficients estimated for cryptophytes are lower limits). Nevertheless, relative comparison of $\bar{a}^*$ and $\bar{a}^*_{act}$ for the same taxon can be done. If photoprotective pigments of diatoms (diadinoxanthin and diatoxanthin) are not taken into consideration, the resulting $\bar{a}^*_{act}$ decreases by less 7% for the two chlorophyll concentrations investigated (Table 3). The contribution of alloxanthin in cryptophytes produces a reduction of nearly 20% for the same conditions (Table 3). In other words, about 20% of the absorption by cryptophytes is not efficient for photosynthesis, even though this absorption contributes to light attenuation in the water column.

A comparison between cryptophytes in these polar waters (or more generally in coastal waters) and cyanobacteria in oligotrophic waters can be made. Both contain phycobiliproteins and their main accessory carotenoid (zeaxanthin in cyanobacteria) is believed to be nonphotosynthetic, if not truly photoprotective [*Bidigare et al.*, 1989; *Babin et al.*, 1996]. Therefore, any quantum yield estimate which makes use of true absorption measurements is lowered by the presence of nonphotosynthetic pigments [e.g., *Bidigare et al.*, 1989; *Lindley et al.*, 1995; *Babin et al.*, 1996]. In (3), the Ψ^* taxonomic differences recorded between diatoms and cryptophytes could be principally due to differences in efficiency (Φ^*) resulting from changes in photosynthetic performance. For cryptophytes, these reductions in efficiency could be partly due to the contribution of the nonphotosynthetic alloxanthin.

Conclusions

The present study shows that for coastal Antarctic waters, the product of integrated chlorophyll content by surface irradiance is, to a first order, a good predictor for daily integrated rates of primary production. Given the weak influence of terrigeneous substances on the optical properties of these waters, a constant value for Ψ^* of 0.07 m^2 g Chl a^{-1} may therefore provide reasonable estimates of primary production for the Southern Ocean, using light and chlorophyll fields. Analysis of the variability of Ψ^*, however, has highlighted the importance of incident light variations, driven by seasonality and cloudiness. The remainder of the variability (more than a factor of 2) can be explained by changes in phytoplankton composition and associated photophysiology.

It was indeed very clear from this study that the water column efficiency in trapping and converting solar energy into organic matter is greater when diatoms dominate the community as compared to cryptophytes or other flagellate species. This observation is restricted to the present data set, but it nevertheless emphasizes the need to account for taxonomic differences in the development of future biooptical models, if the goal is improved accuracy in primary production estimates. Incorporation of the taxon level in these models is another way, albeit not basically different, to partition the open ocean in biogeochemical provinces where specific parameterization may be applied [*Platt and Sathyendranath*, 1991]. There are a number of studies which make the discrimination of phytoplankton taxa by optical techniques a likely outcome in the future. For example, combined information on temperature and water color by remote sensing may allow tracking of new production [*Sathyendranath et al.*, 1991], particularly in upwelling systems [*Dugdale et al.*, 1989]. The dominance of diatoms over other phytoplankton taxa in these productive areas is now widely acknowledged [*Chisholm*, 1992; *Claustre*, 1994]. Blooms of coccolithophorids (e.g., *Emiliania huxleyi*), as often observed in the North Atlantic, may be discriminated from other taxa by the high reflectance generated by their coccoliths [*Balch et al.*, 1989]. Finally, the particular case of cryptophyte-dominated and of phycobiliprotein algae-dominated communities in general may certainly be treated in the future in a more efficient way. Given their particular pigmentation, these phytoplankton will be easily distinguishable from other groups by optical techniques. Moreover, the primary carotenoids of these algae are believed to be nonphotosynthetic. With the goal of improving the accuracy of biooptical models, these particular characteristics may be accounted for by using two different absorption spectra : (1) to propagate the light with depth, the use of an absorption spectra relevant to these phytoplankton groups rather than a standard spectrum may be more accurate, and (2) to account for light utilizable for photosynthesis, scaled fluorescence excitation spectra could be used as an alternative method [*Sakshaug et al.*, 1991]. Consideration of the photophysiological and biooptical peculiarities of taxonomic groups to improve biooptical production models is a promising area of study, even at a global scale.

Acknowledgments. N. Boucher, B. Bozcar, T. Diem, T. Evens, B. Golden, P. Handley, R. Jovine, H. Matlick, T. Newberger, S. Roll, K. Seydel, K. Scheppe, O. Schofield, J. Standish, B. Sullivan, T. Westerberry, ASA personnel at Palmer Station, and the crew of the R/V *Polar Duke* are acknowledged for their assistance in data collection during the three field seasons. We thank R. Bidigare and M. Ondrusek for generously providing pigment standards and D. Antoine for computation of clear-sky irradiance data. H.A. Matlick is acknowledged for his assistance in data analyses and editorial comments. Discussions with A. Morel were greatly appreciated. This study was supported by National Science Foundation grant DPP 90-901127 to B. B. Prézelin. H. Claustre received a NATO grant as part of his sabbatical in B. B. Prézelin laboratory.

References

Antoine, D., and A. Morel, Oceanic primary production 1. Adaptation of a spectral light-photosynthesis model in view of application to satellite chlorophyll observations, *Global Biogeochem. Cycles*, *10*, 43-55, 1996.

Arrigo, K. R., Impact of ozone depletion on phytoplankton growth in the Southern Ocean: large-scale spatial and temporal variability. *Mar. Ecol. Prog. Ser.*, *114*, 1-12, 1994.

Arrigo, K. R., and C. R. McClain, Spring phytoplankton production in the western Ross Sea, *Science*, *266*, 261-262, 1994.

Babin, M., A. Morel, P. G. Falkowski, H. Claustre, A. Bricaud, and Z. Kolber, Nitrogen- and irradiance-dependent variations of the maximum quantum yield of carbon fixation in eutrophic, mesotrophic and oligotrophic marine systems, *Deep Sea Res., Part I*, *43*, 1241-1272, 1996.

Balch, W. M., and C. F. Byrne, Factors affecting the estimate of primary production from space, *J. Geophys. Res.*, *99*, 7555-7570, 1994.

Balch, W. M., R. W. Eppley, M. R. Abbot, and F. M. H. Reid, Bias in satellite-derived pigment measurements due to coccolithophorids and dinoflagellates, *J. Plankton Res.*, *11*, 575-581, 1989.

Bidigare, R. R., O. Schofield, and B. B. Prézelin, Influence of zeaxanthin on quantum yield of photosynthesis of *Synechococcus* clone WH7803 (DC2), *Mar. Ecol. Prog. Ser.*, *56*, 177-188, 1989.

Bidigare, R. R., M. E. Ondrusek, J. H. Morrow, and D. A. Kiefer, *In vivo* absorption properties of algal pigments, in *Ocean Optics* 10, *Proc. SPIE Int. Soc. Opt. Eng.*, *1302*, 290-302, 1990.

Bidigare R. R., B. B. Prézelin, and R. C. Smith, Bio-optical models and the problems of scaling, in *Primary Productivity and Biogeochemical Cycles in the Sea,* edited by P. G. Falkowski and A. D. Woodhead, pp. 175-212, Plenum, New York, 1992.

Bidigare, R. R., J. L. Iriarte, S.-H. Kang, D. Karentz, M. E. Ondrusek, and G.A. Fryxell, Phytoplankton: Quantitative and qualitative assesments, in *Foundations for Ecological Research West of the Antarctic Peninsula,* edited by R. M. Ross, E. E. Hofmann and L. B. Quentin, *Antarct. Res. Ser.*, vol. 70, AGU, Washington, D.C., in press, 1996.

Boucher, N. P., and B. B. Prézelin, Spectral modeling of UV inhibition of *in situ* Antarctic primary production using a newly derived biological weighting function, *Photochem. Photobiol., 64,* 407-418, 1996.

Bricaud, A., M. Babin, A. Morel, and H. Claustre, Variability in the chlorophyll-specific absorption coefficients of natural phytoplankton: analysis and parametrization, *J. Geophys. Res., 100,* 13,321-13,332, 1995.

Buma, A. G. J., N. Bano, M. J. Veldhuis, and G. W. Kraay, Comparison of the pigmentation of two strains of the prymnesiophyte *Phaeocystis sp., Neth. J. Sea Res., 27,* 137-182, 1991.

Bustillos-Guzman, J., H. Claustre, and J.-C. Marty, Specific phytoplankton signature and their relationship to hydrographic conditions in the coastal northwestern Mediterranean Sea, *Mar. Ecol. Prog. Ser., 124,* 247-258, 1995.

Campbell, J. W., and J. E. O'Reilly, Role of satellites in estimating primary productivity on the northwestern Atlantic continental shelf, *Cont. Shelf Res., 8,* 179-204, 1988.

Chisholm, S.W., Phytoplankton size, in *Primary Productivity and Biogeochemical Cycles in the Sea,* edited by P. G. Falkowski and A. D. Woodhead, pp. 213-237, Plenum, New York, 1992.

Claustre, H., The trophic status of various oceanic provinces as revealed by phytoplankton pigment signature, *Limnol. Oceanogr., 39,* 1207-1211, 1994.

Claustre, H., and J.-C. Marty, Specific phytoplankton biomasses and their relation to primary production in the Tropical North Atlantic, *Deep Sea Res., Part I, 42,* 1475-1493, 1995.

Cleveland, J. S., M. J. Perry, D. A. Kiefer, and M .C. Talbot, Maximum quantum yield of photosynthesis in the northwestern Sargasso Sea, *J. Mar. Res., 47,* 869-886, 1989.

Comiso, J. C., C. R. McClain, C. W. Sullivan, J. P. Ryan, and C. L. Leonard, Color Scanner pigment concentrations in the Southern Ocean and relationships to geophysical surface features, *J. Geophys. Res., 98,* 2419-2451, 1993.

Dugdale, R. C., A. Morel, A. Bricaud, and F. P. Wilkerson, Modeling new production in upwelling centers: A case study of modeling new production from remotely sensed temperature and color, *J. Geophys. Res., 94,* 18,119-18,132, 1989.

Falkowski, P. G., Light-shade adaptation and assimilation numbers, *J. Plankton Res., 3,* 203-216, 1981.

Gieskes, W. W. C., and G. W. Kraay, Dominance of cryptophyceae during the phytoplankton spring bloom in the central North Sea detected by HPLC analysis of pigments. *Mar. Biol. Berlin, 75,* 179-185, 1983.

Gieskes, W. W. C., G. W. Kraay, A. Nontji, D. Setiapermana, and Sutomo, Monsoonal alternation of a mixed and a layered structure in the phytoplankton of the euphotic zone of the Banda Sea (Indonesia): a mathematical analysis of algal pigment fingerprints, *Neth. J. Sea Res., 22,* 123-137, 1988.

Holm-Hansen, O., and B. G. Mitchell, Spatial and temporal distribution of phytoplankton and primary production in the western Bransfiled Strait region. *Deep Sea Res., Part A, 38,* 961-980, 1991.

Jeffrey, S. W., A report of green algal pigments in the Central North Pacific Ocean, *Mar. Biol. Berlin, 26,* 101-110, 1976.

Kiefer, D. A., and B. G. Mitchell, A simple, steady state description of phytoplankton growth based on absorption cross section and quantum efficiency, *Limnol. Oceanogr., 24,* 664-672, 1983

Lewis, M. R., Satellite ocean color observations of global biogeochemcial cycles, in *Primary Productivity and Biogeochemical Cycles in the Sea,* edited by P. G. Falkowski and A. D. Woodhead, pp. 139-153, Plenum, New York, 1992.

Li, W. K. W., Photosynthetic response to temperature of marine phytoplankton along a latitudinal gradient (16°N to 74°N), *Deep Sea Res., Part A, 32,* 1381-1391, 1985.

Lindley, S. T., R. R. Bidigare, and R. T. Barber, Phytoplankton photosynthesis parameters along 140 W in the equatorial Pacific. *Deep Sea Res., Part II, 42,* 441-463, 1995.

Marra, J., and R. R. Bidigare, The question of a nutrient effect on the bio-optical properties of phytoplankton, in *Ocean Optics 12, Proc. SPIE Int. Soc. Opt. Eng., 2258,* 153-162, 1994.

Martin, J.H., S. E. Fitzwater, and R. M. Gordon, Iron defficiency limits phytoplankton growth in Antarctic waters, *Global Biogeochem. Cycles, 4,* 5-12, 1990a.

Martin, J.H., S. E. Fitzwater, and R. M. Gordon, Iron in Antarctic waters, *Nature, 345,* 156-158, 1990b.

Mitchell, B. G., and O. Holm-Hansen, Bio-optical properties of Antarctic Peninsula waters: Differentiation from temperate ocean models, *Deep Sea Res., Part A,* 38, 1009-1028, 1991.

Mitchell, B. G., E. A. Brody, O. Holm-Hansen, C. McClain, and J. Bishop. Light limitation of phytoplankton biomass and macronutrient utilization in the Southern Ocean, *Limnol. Oceanogr.*, 36, 1662-1677, 1991.

Moline, M. A., and B. B. Prézelin, High-resolution time-series data for primary production and related parameters at a Palmer LTER Coastal site: implications for modeling carbon fixation in the Southern Ocean, *Polar Biol.*, in press, 1996a.

Moline, M. A., and B. B. Prézelin, Palmer LTER 1991-1994: Long-term monitoring and analyses of physical factors regulating variability in coastal Antarctic phytoplankton biomass, *in situ* productivity and taxonomic composition over subseasonal, seasonal and interannual time scales, *Mar. Ecol. Prog. Ser.*, in press, 1996b.

Morel, A., Available, usable, and stored radiant energy in relation to marine photosynthesis, *Deep Sea Res., 25,* 675-688, 1978.

Morel, A., Optical modeling of the upper ocean in relation to its biogeneous matter content (case I waters), *J. Geophys. Res., 93,* 10,749-10,768, 1988.

Morel, A., Light and marine photosynthesis: A spectral model with geochemical and climatological implications, *Prog. Oceanogr., 26,* 263-306, 1991.

Morel, A., and R. C. Smith, Relation between total quanta and total energy for aquatic photosynthesis, *Limnol. Oceanogr., 19,* 591-600, 1974.

Morel, A., D. Antoine, M. Babin, and Y. Dandonneau, Measured and modeled primary production in the Northeast Atlantic (Eumeli JGOFS program): The impact of natural variations in photosynthetic parameters on model predictive skill, *Deep Sea Res., Part I, 43,* 1273-1304, 1996.

Neale, P. J., and P. J. Richerson, Photoinhibition and the diurnal variation of phytoplankton photosynthesis, I, development of a photosynthesis-irradiance model from studies of *in situ* responses, *J. Plankton Res., 9,* 167-193, 1987.

Platt, T., Primary production of the ocean water column as a function of surface light intensity: Algorithms for remote sensing, *Deep Sea Res., Part A, 33,* 149-163, 1986.

Platt, T., and S. Sathyendranath, Oceanic primary production: Estimation by remote sensing at local and regional scales, *Science, 241,* 1613-1620, 1991.

Platt, T., and S. Sathyendranath, Estimators of primary production for interpretation of remotely sensed data on ocean color, *J. Geophys. Res., 98,* 14,561-14,576, 1993.

Prasad, K. S., S. E. Lohrenz, D. G. Redalge, and G. L. Fahnenstiel, Primary production in the Gulf of Mexico coastal waters using "remotely-sensed" trophic category approach, *Cont. Shelf Res., 15,* 1355-1368, 1995.

Prézelin, B. B., N. P. Boucher, M. A. Moline, E. Stephens, K. Seydel and K. Scheppe, Palmer LTER program: spatial variability in phytoplankton distribution and surface photosynthetic potential within the peninsula grid, november 1991, *Ant. J. U. S., 27,* 242-245, 1992.

Priddle, J., R. B. Heywood, and E. Theriot, Some environmental factors influencing phytoplankton in the Southern Ocean around South Georgia, *Polar Biol., 5,* 65-79, 1986.

Rivkin, R. B., and M. Putt, Seasonal pattern of diel periodicity in photosynthesis by polar phytoplankton : species-specific responses, *J. Phycol., 24,* 369-376, 1988.

Ross, R. M., and L. B. Quentin, Palmer long-term ecological research (LTER): An overview of the 1991-1992 season, *Ant. J. U. S., 27,* 235-236, 1992.

Rowan, K. S. (Ed.), Photosynthetic Pigments of Algae, Cambridge Univ. Press, New-York, 1989.

Sakshaug, E., G. Johnsen, K. Andresen, and M. Vernet, Modeling of light-dependent algal photosynthesis and growth: Experiments with the Barents Sea diatoms *Thalassiosira nordenskioeldii* and

Chaetoceros furcellatus, Deep Sea Res., 38, Part A, 415-430, 1991.

Sathyendranath, S., T. Platt, E. P. W. Horne, W. G. Harrison, O. Ulloa, R. Outerbride, and N. Hoepffner, Estimation of new production in the ocean by compound remote sensing, *Nature, 353*, 129-133, 1991.

Schofield, O., B. B. Prézelin, R. R. Bidigare, and R. C. Smith, *In situ* photosynthetic quantum yield. Correspondence to hydrographic and optical variability within the Southern California Bight, *Mar. Ecol. Prog. Ser., 93*, 25-37, 1993.

Siegel, D. A., A. F. Michaels, J. C. Sorensen, M. C. O'Brien, and M. A. Hammer, Seasonal variability of light availability and utilization in the Sargasso Sea, *J. Geophys. Res., 100*, 8695-8713, 1995.

Smith, R. C., et al., Ozone depletion: Ultraviolet radiation and phytoplankton biology in Antarctic waters. *Science, 255*, 952-959, 1992.

Smith, R. C., et al., The palmer LTER: A long-term ecological research program at Palmer Station, Antarctica, *Oceanography, 8*, 77-86, 1996a.

Smith, R. C., H. Dierssen, and M. Vernet, Phytoplankton biomass and productivity in the western Antarctic peninsula region in *Foundations for Ecological Research West of the Antarctic Peninsula*, edited by R. M. Ross, E. E. Hofmann and L. B. Quentin, *Antarct. Res. Ser.*, vol. 70, AGU, Washington, D.C., in press, 1996b.

Smith, W. O., Jr., and E. Sakshaug, Polar Phytoplankton, in *Polar Oceanography, Part B: Chemistry, Biology and Geology*, pp. 477-525, Academic, San Diego, Calif., 1990.

Sullivan, C. W., K. R. Arrigo, C. R. McClain, J. C. Comiso, and J. Firestone, Distributions of phytoplankton blooms in the Southern Ocean, *Science, 262*, 1832-1837, 1993.

Tilzer, M. M., and Z. Dubinsky, Effects of temperature and daylength on the mass balance of Antarctic phytoplankton, *Polar Biol., 7*, 35-42, 1987.

Tilzer, M. M., M. Elbrätcher, W. W. C. Gieskes, and B. Beese, Light-temperature interactions in the control of photosynthesis in Antarctic Phytoplankton, *Polar Biol., 5*, 105-111, 1985.

Vaulot, D., J.-L. Birrien, D. Marie, R. Casotti, M. J. Veldhuis, G. W. Kraay, and M.-J. Chrétiennot-Dinet, Morphology, ploidy, pigment compoistion, and genome size of cultured strains of *Phaeocystis* (Prymnesiophyceae), *J. Phycol., 30*, 1022-1035, 1994.

Waters, K. J., and R. C. Smith, Palmer LTER: A sampling grid for the Palmer LTER program, *Ant. J. U. S., 27*, 236-239, 1992.

Whitaker, T. M., Primary production of phytoplankton off Signy Island, South Orkneys, the Antarctic, *Proc. R. Soc. London A, 214*, 169-189, 1982.

Wozniak, B., J. Dera, and O. Koblentz-Mischke, Modeling the relationship between primary production, optical properties and nutrients in the sea (as a basis for indirectely estimating primary production). in *Ocean Optics 11, Proc. SPIE Int. Soc. Opt. Eng., 1750*, 246-275, 1992.

Wright, S.W., and S. W. Jeffrey, Fucoxanthin markers of marine phytoplankton analysed by HPLC and HPTLC, *Mar. Ecol. Prog. Ser., 38*, 259-266, 1987.

Wright, S. W., S. W. Jeffrey, R. F. C. Mantoura, C. A. Llewellyn, T. Bjørnland, D. Repeta, and N. Welschmeyer, Improved HPLC method for the analysis of chlorophylls and carotenoids from marine phytoplankton, *Mar. Ecol. Prog. Ser., 77*, 183-196, 1991.

Yoder, J. A., L. P. Atkinson, S. S. Bishop, J. O. Blanton, T. N. Lee, and L. J. Pietrafesa, Phytoplankton dynamics within Gulf Stream intrusions on the southeastern United States continental shelf during summer 1981, *Cont. Shelf Res., 4*, 611-635, 1985.

Zimmerman, R. C., J. B. SooHoo, J. N. Kremer, and D. Z. D'Argenio, Evaluation of variance approximation techniques of non-linear photosynthesis-irradiance models, *Mar. Biol. Berlin, 95*, 209-215, 1987.

H. Claustre, Laboratoire de Physique et Chimie Marines, CNRS-INSU, B.P. 08, 06230 Villefranche-sur-mer, France. (e-mail: Claustre@ccrv.obs-vlfr.fr)

M. A. Moline and B. B. Prézelin, Department of Ecology, Evolution, and Marine Biology, University of California at Santa Barbara, Santa Barbara, CA 93106.

(Received June 6, 1996; accepted August 5, 1996.)